Brain Structure and Function (2019) 224:2437–2452
https://doi.org/10.1007/s00429-019-01913-w

ORIGINAL ARTICLE

Top-down control of the medial orbitofrontal cortex to nucleus accumbens core pathway in decisional impulsivity

Zhiyan Wang[1] · Lupeng Yue[1] · Cailian Cui[1] · Shuli Liu[1] · Xuewei Wang[1] · Yijing Li[1] · Longyu Ma[1]

Received: 2 July 2018 / Accepted: 14 June 2019 / Published online: 1 July 2019

Abstract

Decisional impulsivity is one of the risk factors for occurrence and development of many mental disorders, and that the dysfunctions of orbitofrontal cortex (OFC) and nucleus accumbens core (NAcC) are at least involved. Although previous studies have shown that the role of OFC as a whole in regulating decision-making impulse behavior is inconsistent, it's still unclear that the roles of the subregions of OFC including their projections to the NAcC in decisional impulsivity. The present study was designed to investigate the roles of OFC subregions, medial OFC (mOFC) and lateral OFC (lOFC) and their projections to the NAcC in decisional impulsivity in free-moving rats. We found that rats with low level of decisional impulsivity (LI) showed higher neuronal activity in both the mOFC and lOFC, and more neurons in mOFC but not lOFC projecting to the NAcC were activated, compared with high level of decisional impulsivity (HI) rats. The mOFC-NAcC projections of LI rats showed stronger information communication in beta and low gamma oscillations in the expected reward choice and delay time windows. Further, specific activation (in HI rats) or inhibition (in LI rats) of the mOFC-NAcC pathway could partly reverse their decisional impulsive behaviors. The findings first demonstrated that the mOFC-NAcC pathway was more important than the lOFC-NAcC pathway to the top-down control in decisional impulsivity, which could be a new neural physiological mechanism for psychiatric disorders associated with decisional impulsivity.

Keywords Decisional impulsivity · Medial orbitofrontal cortex (mOFC) · Nucleus accumbens core (NAcC) · High decisional impulsivity (HI) · Low decisional impulsivity (LI)

Introduction

Usually, proper decision-making of individuals depends on their assessment of the external stimulus that they faced and the choices they made to deal with it. Decisional impulsivity is an internal decision-making process and is simply described as "actions initiated without due deliberation of other possible options or outcomes behaviors" (Dalley et al. 2008). Thus, decisional impulsivity is one of an individual's specific personality traits. The levels of decisional impulsivity could be divided into high (HI), middle (MI), and low (LI) according to certain criteria. The HI and LI are regarded as trait-like decisional impulsivity (Caprioli et al. 2014). HI are reported in attention-deficit/hyperactivity disorder (ADHD) (Patros et al. 2016; Metin et al. 2016), obsessive–compulsive disorder (OCD) (Sohn et al. 2014), and substance addiction (Diergaarde et al. 2008; Harvey-Lewis et al. 2012). LI are displayed in individuals with high-lethality suicide attempts (Dombrovski et al. 2011). Moreover, HI rats acquired cocaine self-administration at a significantly faster rate than the LI rats (Perry et al. 2005). Therefore, the trait-like decisional impulsivity is often considered as risk factors for the occurrence and development of psychiatric disorders.

Although the neural mechanisms of decisional impulsivity are not quite clear, previous studies have shown that functional abnormalities in the orbitofrontal cortex (OFC) is involved (Berlin et al. 2004; Darna et al. 2015). Patients with

Electronic supplementary material The online version of this article (https://doi.org/10.1007/s00429-019-01913-w) contains supplementary material, which is available to authorized users.

✉ Cailian Cui
clcui@bjmu.edu.cn

[1] Department of Neurobiology, School of Basic Medical Sciences, Key Laboratory for Neuroscience of the Ministry of Education and National Health and Family Planning Commission Neuroscience Research Institute, Peking University Health Science Center, 38 Xue Yuan Road, Beijing 100191, China

OFC damage prefer immediate rewards and display high levels of decisional impulsivity (Bechara et al. 2000; Besson et al. 2010). However, rats with whole OFC lesions show inconsistent results in different studies, some rats prefer the small-immediated reward (Mobini et al. 2002; Rudebeck et al. 2006), while others prefer the large-delayed reward (Winstanley et al. 2004). The OFC consists of different subregions, including medial OFC (mOFC) and lateral OFC (lOFC). A study has indicated that dissociable effects of lesions to mOFC and lOFC on impulsive choice in rats (Mar et al. 2011). Besides, evidence has proven repeatedly that rats with nucleus accumbens core (NAcC) lesions or inactivation prefer the small-immediate reward and increase the level of decisional impulsivity (Bezzina et al. 2007; Cardinal et al. 2001; Pothuizen et al. 2005). Obviously, the dysfunctions of OFC and NAcC are at least involved in decisional impulsivity. However, it's still unclear whether the subregions of OFC and the projections from them to the NAcC play different roles in decisional impulsivity.

In addition, the neurons in the OFC are necessary for guiding behavior based on the value of expected reward outcomes (Izquierdo et al. 2004) and encode the value of offered and chosen goods, which is independent of visuospatial factors and motor responses (Padoa-Schioppa and Assad 2006). Furthermore, a minority of neurons in the OFC exhibit sustained increases in firing in anticipation of reward delay time (Roesch et al. 2006). These results indicate that the OFC neurons are associated with the encoding of reward value and its delay time. However, it is also unknown whether the neuron projections of the mOFC-NAcC and lOFC-NAcC could be involved in these processes.

In view of the above, we speculate that the neuron projections from the mOFC or lOFC to NAcC may play a top-down control role in decisional impulsivity via encoding of reward value and its delay time. In the present work, neuron-projected tracing, in vivo multi-channel recording and chemogenetic technologies were used in free-moving trait-like decisional impulsivity rats to test the hypothesis.

Materials and methods

A total of 132 male Sprague–Dawley rats (Animal Center of Peking University, China) were trained in the delay-discounting task and 65 rats were selected as trait-like decisional impulsive rats, $n = 31$ HI rats and $n = 34$ LI rats, respectively. All rats weighed 220–250 g at the start of experiments and were habituated to the environment for 1 week before training. Each rat was housed individually, maintained on a 12:12-h light–dark cycle (lights off at 06:30 a.m.). The room temperature was controlled at 22 ± 3 ℃, and the relative humidity was $60 \pm 15\%$. Food was available ad libitum, but water was restricted on the training days. The rats were allowed to freely drink water for 15 min after training, and each rat obtained 40–50 ml of water per day, which was enough for their daily need. Rats were trained 5 or 6 days per week. All experiments met the requirements of National Institute of Health Guide for the Care and Use of Laboratory Animals (National Research Council 1996), and the procedures were approved by the Animal Use Committee of Peking University Health Science Center (Approval Number: LA2010-53) in our study.

Behavioral apparatus and training

Training took place in the operant chambers (40 cm × 20 cm × 40 cm) equipped with a 6-W house light above and two retractable levers in one sidewall. The levers were 4 cm wide, 5 cm from the plexiglas floor and 10 cm apart, and equally distant to the sidewall. A metal disk for water, which was 2 cm from the floor, was located in the center between the two levers. A pump delivered the water reward (40 µl per drop). A computer programmed the chambers and collected the behavioral data.

The delay discounting task was modified from the experiment model by Zuo et al. (2012). First, rats learned to trigger a lever (counterbalanced across group) and press the lever for water reward. Second, they were trained to perform the task until a stable behavioral performance was achieved. Daily behavioral training consisted of six blocks and lasted for 45 min approximately. Each block consisted of twelve trials. Within each block, the first two trials were forced choice, in which only one lever extended (either right or left, counterbalanced in the group), and the remaining ten trials were free choice, in which both the two levers extended. The house light on signaled the beginning of each trial, and the levers extended 2 s later. In the forced trials, rats must press the extended lever to obtain the corresponding reward. In the free trials, rats were required to respond on either lever within 10 s. Responding on one lever (right or left) resulted in small-immediate reward (one drop of water), and responding on the other lever resulted in large-delayed reward after different delays across blocks (five drops of water) (left or right, counterbalanced in the group). Then the levers retracted and rats waited for the corresponding reward delivery. The house light remained on during the delay period and was off after the reward delivery. The trial ended and entered into the inter-trial interval (ITI) time until the start of next trial. If rats did not respond to the levers within 10 s in free-choice trials, it directly entered into the ITI and this trial was recorded as an omission. The levers associated with the large and small reward were always the same for each rat during the whole training and experiments. The small reward remained 2 s delay within all blocks and the delay to large reward increased from 2 to 4, 8, 12, 16 and 20 s across blocks. The ITI duration was [40–response latency + delay duration)] seconds.

A stable baseline behavioral performance was defined as: repeated measures ANOVA analysis of behavioral data from the last three consecutive sessions showed that the main effect of 'session' was not significant, and the effect of 'delay' was significant at $p < 0.05$ level (Li et al. 2015).

Retrograde tracer and immunofluorescence

In the retrograde tracer experiments, four HI rats and four LI rats were anesthetized with 40 mg/kg sodium pentobarbital (i.p.) and then were secured in a stereotaxic apparatus. The FG (Weiner 2008) (4%, Fluorochrome, 0.5 µl) was delivered unilaterally into the NAcC (anteroposterior − 1.6 ~ 1.8 mm from bregma, mediolateral 1.8 mm, and dorsoventral − 6.8 mm from dura) over 5 min with a syringe pump directly connected to Hamilton syringes. Then, the syringe was left in place for an additional 2 min to allow FG to diffuse in the local vicinity of the injector tip (Ge et al. 2017). The animals were retrained after one-week recovery from the surgery.

In the immunohistochemical experiments, the delay-discounting task was 45 min and all animals were perfused 45 min later. HI and LI rats were deeply anesthetized with chloral hydrate (350 mg/kg, i.p.). Then they were perfused with 300 ml of 0.9% saline, followed by 400 ml of 4% PFA in 0.1 M PBS (pH = 7.4). The stripped brains were fixed in 4% PFA for 24 h, then transferred to 30% sucrose in PBS for dehydration. The brain slices of NAc were chosen from anteriorposterior + 1.7 to +1.4, and that of OFC were chosen from anteriorposterior + 4.1 to + 3.8 to be used slicing. Each brain slice was 30 µm. One of every five slices was taken, and a total of 6 slices were obtained from the NAc or OFC of each rat for double-label or triple-label staining. All brain slices were kept in cryoprotectant (20% glycerol, 30% ethylene glycol and 2% DMSO in 0.1 M PBS, pH 7.4) and stored at − 80 °C until further processing.

For the immunofluorescence, the free-floating brain slices were first rinsed in PBS, permeabilized in PBS with 0.3% Triton X-100 (PBS-Tx) for 30 min, then were blocked with PBS-Tx containing 5% normal donkey serum for 1 h. The primary antibody was diluted in 1% normal donkey serum in PBS-Tx and the slices were incubated overnight at 4 °C. The following primary antibodies were used in our study: rabbit anti-c-Fos (1:500; Santa Cruz Biotechnology; sc-52); mouse anti-NeuN (1:800; Millipore; MAB377); and rabbit anti-FG (FG injection site, 1: 10,000; Millipore; AB153). On the second day, the slices were rinsed in PBS-Tx and then were incubated for 1 h with the following secondary antibodies: Alexa Fluor 488 donkey anti-rabbit IgG (c-Fos, 1:500; Invitrogen; A21206) and Alexa Fluor 555 donkey anti-mouse IgG (1:500; Invitrogen; A31570). Finally, the slices were rinsed with PBS again, mounted onto slides, and coverslipped with the anti-fade solution (Applygen Technologies Inc). The stained brain slices were photographed under an Olympus FV1000 confocal microscope (Olympus Corporation) using 10X, 20X or 40X objectives. It is worth noting that the FG was visualized using confocal microscopy without incubating the FG primary antibody to avoid cross-reactivity, as anti-c-Fos and anti-FG were both raised in rabbit. What's more, detection of FG without additional histochemical processing allowed for identification and dissection of FG-labeled regions under UV light when tissues were processed with neutral pH buffer (Weiner 2008). After the histochemistry staining, four views of each site were chosen randomly in each slice for immunohistochemical analysis. The labeling cells were counted by averaging the results from two persons using the same criteria, such as the same site of each view, the same labeling-cell brightness, and conducted in a blind manner.

Virus injection, cannula implantation and microinfusions

In the chemogenetic experiments, sixteen HI and eighteen LI rats were microinjected with virus into mOFC (anteriorposterior + 4.0 mm from bregma, mediolateral ± 0.5 mm, dorsoventral − 3.7 mm from dura). The microinjection protocols were similar to the FG injections described above. The AAV5-CaMKII-hM3D(Gq)-mCherry (hM3Dq) or AAV5-CaMKII-mCherry (mCherry) (0.5 µl per side, Vector Core, University of North Carolina) was microinjected bilaterally into mOFC of HI rats, while the AAV8-hSyn-hM4d (Gi)- mCherry (hM4Di) or AAV5-Syn-mCherry (mCherry) (0.5 µl per side, Vector Core, University of North Carolina) was microinjected bilaterally into mOFC of LI rats. The animals started to be retrained 1 week later and the virus was fully expressed in the terminals of the NAcC neurons after 6 weeks.

Guide cannulas were implanted bilaterally into NAcC 2 weeks before the CNO injections. HI and LI rats were anesthetized with 40 mg/kg sodium pentobarbital (i.p.) and their heads were fixed to a stereotaxic apparatus with the incisor bar set at − 3.3 mm for a flat skull position. Bilateral stainless-steel guide cannulas (OD 0.64 mm) were implanted into NAcC according to the following stereotaxic coordinates: anteroposterior − 1.6 ~ 1.8 mm from bregma, mediolateral ± 1.8 mm, and dorsoventral − 5.3 mm from dura. The cannulas were secured to the skull using three bone screws and dental cement. The tips of the guide cannulas were 1.5 mm above the intended sites of injection. Internal cannulas were replaced with dummy cannulas, which were 0.5 mm longer than guide cannulas, to keep the cannulas patent and prevent infection. After surgery, rats were housed individually and rested for 1 week. Following the recovery period, rats were retrained in the delay-discounting task.

During the infusions, rats moved freely whilst the internal cannula was removed and an injector extending 1.5 mm

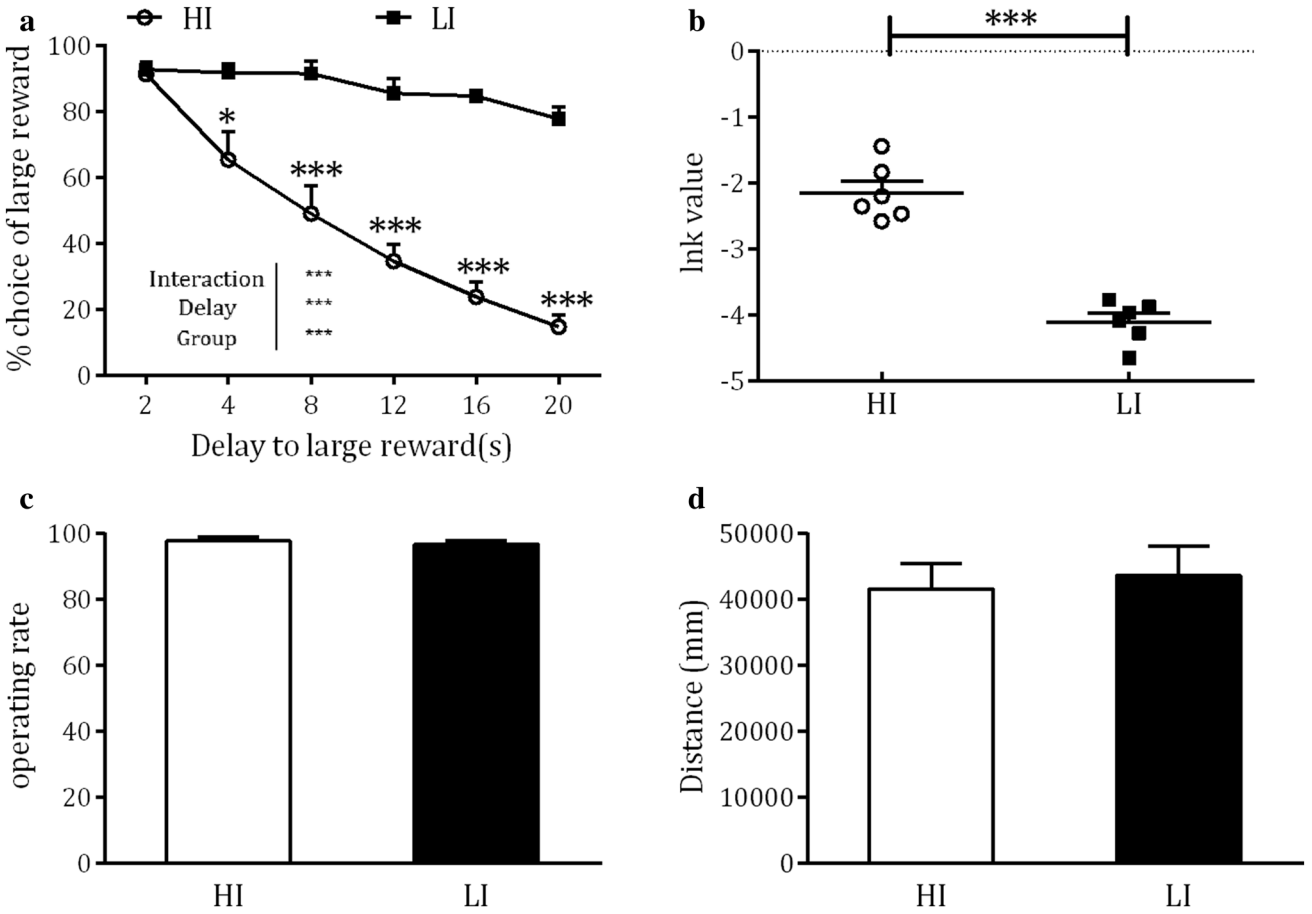

Fig. 1 Behavioral performance of HI and LI rats in delay discounting task. **a** Significant choice percentage of large reward was in HI and LI rats. Two-way ANOVA showed a significant group (HI, LI), delay (2, 4, 8, 12, 16, 20 s) and group × delay interaction effect (group: F1, 55 = 26.67, $p < 0.001$; delay: F5, 55 = 46.13, $p < 0.01$; group × delay: F5, 55 = 13.02, $p < 0.01$), and Bonferroni post tests showed significant difference at 4 s, 8 s, 12 s, 16 s and 20 s (4 s, $p < 0.05$; 8 s, 12 s, 16 s, 20 s, $p < 0.001$, respectively). **b** The lnk value of HI rats was significantly higher than that of LI rats (unpaired t test, $p < 0.001$). **c** No significant statistical significance in operating rate between HI and LI rats in all free trails of the delay-discounting task (unpaired t test, $p = 0.60$). **d** The total distance of free movement of LI and HI rats in 30 min was not statistically significant (unpaired t test, $p = 0.74$). HI and LI rats, $n = 6$, respectively. *$p < 0.05$; ***$p < 0.001$, error bars represent mean ± SEM

beyond the length of the guide cannula was inserted. 10 min before the delay-discounting task, vehicle (saline) or CNO (1 mM, 0.4 µl per side; Tocris; 4936) were bilaterally microinjected into the NAcC at a rate of 0.2 µl/min and the injector was left in place for an additional 2 min. Then the injector was removed and replaced with the internal cannula. Rats were put into the operant chambers and the delay-discounting task started 5 min later. Each rat received vehicle and CNO, respectively, in random on two testing days. Before the first testing, half of the HI and LI rats were microinjected with CNO into NAcC using procedures described above, the other half of rats were microinjected with vehicle. During the second test day, the microinjections were reversed. At the end of the second behavioral testing, all rats were sacrificed to verify the cannula placements and the expressions of hM3Dq or hM4Di.

Multi-channel electrode implantation and electrophysiological recordings

Five HI rats and six LI rats were included in the multi-channel recording experiments. Rats were anaesthetized with 40 mg/kg sodium pentobarbital (i.p.) using standard stereotaxic techniques, and two custom-fabricated chromel alloy electrodes were implanted unilaterally into NAcC and mOFC (NAcC, anteroposterior 1.8 mm, mediolateral 1.8 mm, and dorsoventral − 6.8 mm from dura; mOFC, anteriorposterior 4.0 mm, mediolateral 0.6 mm, dorsoventral − 3.7 mm; based on the atlas of Paxinos and Watson (1998)). The NAcC electrodes, of 0.8 mm in length, had two lines, and each line had four recording sites that were 0.2 mm apart (a total of 8 sites per electrode); while the mOFC electrodes also had two lines, each line had 8 recording sites that were 0.2 mm apart (a total of 16 sites per electrode, 1.7 mm in

length). The multi-channel electrodes were implanted at a rate of 0.5 mm/5 min. The ground wire was intertwined to one of the five bone screws and multi-channel electrodes were secured to the bone screws using dental cement. After the surgery, rats were housed individually and rested for 1 week for recovery. Then rats were retrained in the delay-discounting task for electrophysiological recordings. The local field potential (LFP) signals were recorded daily during delay-discounting task performance (the number of sessions recorded in all rats is shown in Online Resource 1_Table 2). The LFPs were recorded by low-pass filtering (0–200 Hz, Cineplex, Plexon Inc, USA) of raw signals and were digitized at 1 kHz. The first 2 min of LFPs before delay-discounting task were regarded as baseline. Then the LFPs were recorded synchronously with rats performing the delay-discounting task. A video tracking system (Cineplex, Plexon Inc, USA) was used to monitor animal performance during the recording.

Statistical analysis

Behavioral and immunohistochemical data analysis

To estimate the level of decisional impulsivity of rats, the k value of the hyperbolic discounting $V = V_0/(1 + k\mathrm{D})$ was calculated, where V was the choice percent of large reward after a delay of D in seconds. V_0 was the choice percent of large reward at Block 1 ($D = 2$ s) and the free parameter k described how rapidly V declines with increasing delay. The calculated k values were too small so they were shown as lnk, which represented the level of decisional impulsivity of rats. The low, middle or high decisional impulsivity (LI, MI, HI) rats were classified into three groups based on the lnk values of the last three sessions of stable behavioral performance (Online Resource 1_Fig. S1). The rats with the highest and lowest quartiles of the lnk values were classified as HI and LI rats.

All data were presented as the mean ± standard error of the mean (SEM). The behavioral data analysis (Fig. 1) was conducted using IBM SPSS (version 20, IBM Corporation, Armonk, NY, USA). As described in detail in previous reports (Bezzina et al. 2007), the choice percentage of large reward, the operating rate of all free trials and the number of omissions were analyzed. Behavioral data were analyzed using single dependent variable factor analysis of variance (ANOVA) with group and delay (three groups, six delays) as factors. The operating rate and the number of omissions were analyzed using unpaired t test or two-way ANOVA and LSD post hoc test. Data from NeuN/c-Fos double staining and c-Fos/NeuN/FG triple staining (Figs. 2, 3) were analyzed with unpaired t-test, followed by Tukey's or Bonferroni's post hoc test. Graphs were produced using GraphPad PRISM 6.0. Statistical significance was set at $p < 0.05$. Only the significant effects that were critical for the data interpretation were reported. During the analysis, the homogeneity of variance across groups was determined using Tamhanes' T2 if the homogeneity of variance of data was not equal.

Electrophysiological data analysis

LFP analysis was performed using Chronux (http://chronux.org/). The bandwidth product was 3, and 5 tapers. LFP signals were fragmented into different segments according to the performance of rats and were filtered at the bandpass of 1−46 Hz and 55–100 Hz to In brief, the two different time series modeled as a form:

$$\begin{bmatrix} x_1(t) \\ x_2(t) \end{bmatrix} = \sum_{r=1}^{p} Ar\left(\begin{bmatrix} x_1(t-r) \\ x_2(t-r) \end{bmatrix} \right) + \begin{bmatrix} u_1(t) \\ u_2(t) \end{bmatrix}$$

[(u1(t), u2(t)] represented the uncorrelated Gaussian white noise processes representing the model residuals, the model order p was determined by the minimum of Akaike Information Criterion or Bayesian Information Criterion.

Generalized partial directed coherence (gPDC) was calculated as previously described (Baccalá and Sameshima 2001; de Brito et al. 2010; Taxidis et al. 2010). This algorithm was based on a multi-variate autoregressive (MVAR) model, which integrated both mOFC and NAcC LFP signals. The gPDC at each frequency was divided into five frequency oscillations: 3–5 Hz (delta), 6–8 Hz (theta), 9–13 Hz (alpha), 15–29 Hz (beta), 30–46 Hz (low gamma) and 55–100 Hz (high gamma). The gPDC was defined as follows:

$$\left| C_{i \leftarrow j}(f) \right| = \frac{a_{ij}(f)}{\sqrt{\sum_k \frac{1}{\sigma_k^2} \left| a_{kj}(f) \right|^2}}.$$

Aij (f) was the Fourier transformation of the MVAR coefficient $\left(\mathrm{Ar} = \begin{bmatrix} \mathrm{a}_{11} & \mathrm{a}_{12} \\ \mathrm{a}_{21} & \mathrm{a}_{22} \end{bmatrix} \right)$, σ_k represented the standard deviation of the model residuals. The gPDC value (Figs. 5, 6) was in the interval of [0 1], where "0" standed for the absence of an influence of a target on the source and "1" standed for a linearly predictable target from the source.

Results

Different activation level of neurons in the mOFC, lOFC and NAcC between HI and LI rats

According to the division standards of lnk values mentioned above, trait-like decisional impulsive rats were screened (Fig. 1a and Online Resource 1_Fig. S1). As the

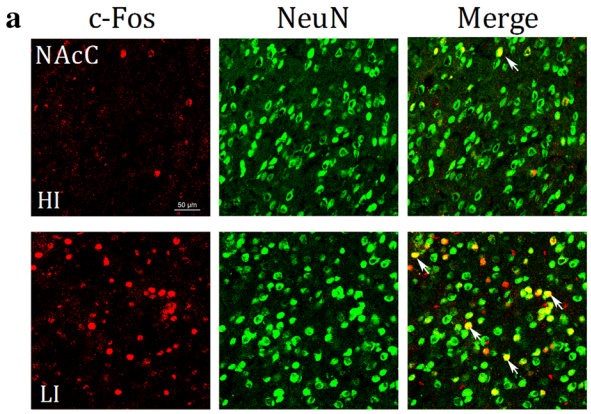
a
c-Fos
NeuN
Merge
NAcC
HI
LI

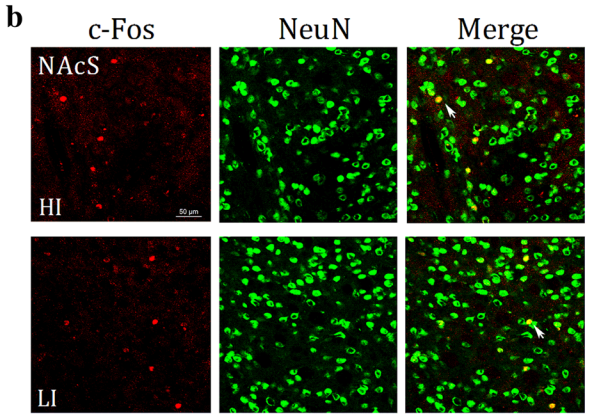
b
c-Fos
NeuN
Merge
NAcS
HI
LI

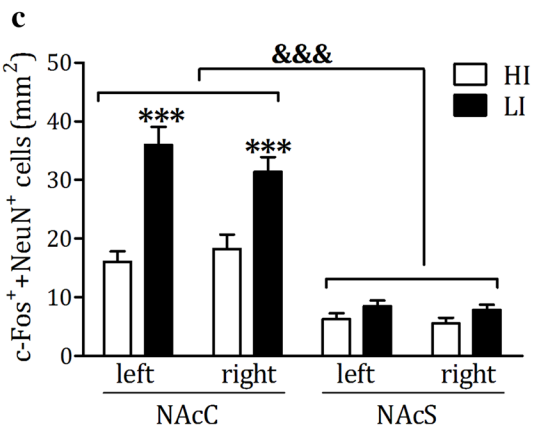
c
&&&
***
***
HI
LI
c-Fos+NeuN+ cells (mm2)
50
40
30
20
10
0
left
right
left
right
NAcC
NAcS

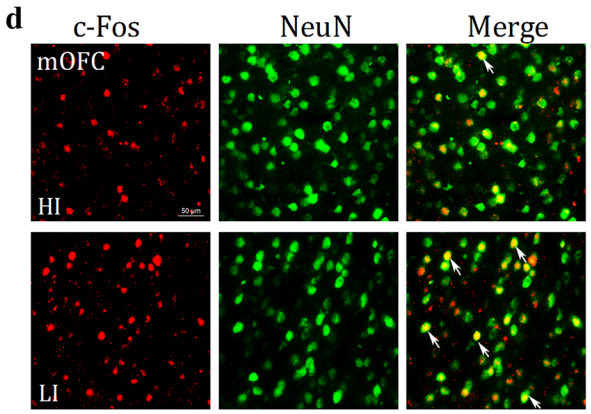
d
c-Fos
NeuN
Merge
mOFC
HI
LI

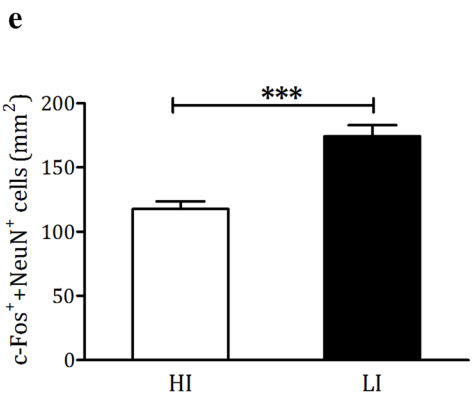
e
***
c-Fos+NeuN+ cells (mm2)
200
150
100
50
0
HI
LI

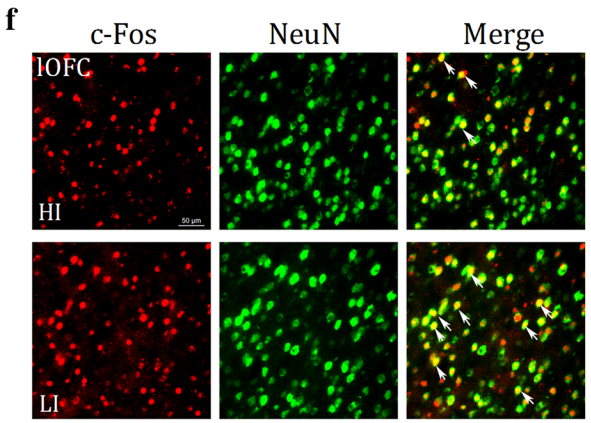
f
c-Fos
NeuN
Merge
lOFC
HI
LI

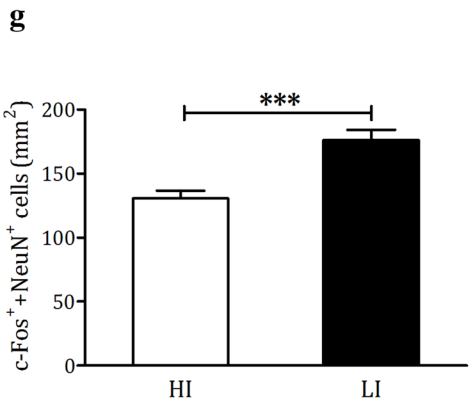
g
***
c-Fos+NeuN+ cells (mm2)
200
150
100
50
0
HI
LI

◂**Fig. 2** Difference of activated neurons in different subregions of the OFC and NAc between HI and LI rats. Representative photomicrographs (20X) of c-Fos (red) and NeuN (green) labeling in the **a** NAcC(a), **b** NAcS, **d** mOFC and **f** lOFC in HI and LI rats after delay-discounting task. Scale bar, 50 μm. Above: HI rats; Below: LI rats. Arrow: examples of c-Fos + NeuN double-positive cells. **c** The number of double-positive cells per mm^2 in NAcC in HI rats was significantly fewer than that in LI rats (unpaired *t* test, left: $p < 0.001$; right: $p < 0.001$). However, that in NAcS had no difference between HI and LI rats (unpaired t test, left: $p = 0.13$; right: $p = 0.079$). Besides, the number of c-Fos+NeuN double-positive cells in NAcC in both HI and LI rats was significantly more than that in NAcS, but no difference in the left or right (two-way ANOVA, subregion: FHI = 29.53, FLI = 57.28, $p < 0.001$, respectively; side: FHI = 0.12, FLI = 0.59, pHI = 0.66, pLI = 0.22). The number of c-Fos+NeuN double-positive cells in the **e** mOFC or **g** lOFC in LI rats was significantly more than that in HI rats (unpaired t test, $p < 0.001$, respectively). HI and LI rats, $n = 4$, respectively. ***$p < 0.001$, &&& $p < 0.001$, error bars represent mean ± SEM

delay of large reward increased, the HI and LI rats had a large difference in choice between large-delayed and small-immediate reward. HI rats preferred the small-immediate reward, while LI rats preferred the large-delayed reward. The difference was especially significant at the 4 s, 8 s, 12 s, 16 s and 20 s delay. The lnk values of HI rats were significantly higher than that of LI rats (HI, -2.14 ± 0.18; LI, -4.10 ± 0.13; Fig. 1b). However, there was no significant difference in operating rate between HI and LI rats throughout all free trials (HI, $97.8 \pm 1.3\%$; LI, $96.9 \pm 1.2\%$; Fig. 1c). Moreover, there was no difference in the total distance of free movement in 30 min between HI and LI rats (HI, 41670 ± 3859 mm; LI, 43670 ± 4520 mm; Fig. 1d). These results suggested that HI and LI rats showed significant difference in the level of decisional impulsivity, but not the level of movement.

To investigate whether the subregions of OFC and NAc played roles in decisional impulsivity, the number of c-Fos/NeuN double-positive cells (per mm^2) were counted in NAcC, NAcS, mOFC and lOFC. The numbers of c-Fos/NeuN double-positive cells in the left and right NAcC in LI rats were both twice of those in HI rats (LI, left, 36.0 ± 3.1, right, 31.4 ± 2.5; HI, left, 16.1 ± 1.8, right, 18.3 ± 2.5; Fig. 2c). However, there was no difference in the number of double-positive cells in the both sides of NAcS between HI and LI rats (LI, left, 8.5 ± 1.0, right, 7.9 ± 0.9; HI, left, 6.3 ± 1.0, right, 5.5 ± 1.0; Fig. 2c). What's more, similar to the NAcC, the number of c-Fos/NeuN double-positive cells in LI rats was more than that of HI rats both in mOFC and lOFC (mOFC, LI, 174.3 ± 8.6; HI, 117.6 ± 6.1; lOFC, LI, 176.0 ± 8.3, HI, 130.5 ± 5.3; Fig. 2e, g). Interestingly, we also found that the number of c-Fos/NeuN double-positive cells in the left and right NAcC was much more than that in NAcS in both HI and LI rats (Fig. 2c).

Together, no matter in the mOFC or lOFC, the significant difference in neuronal expression of c-Fos between trait-like decisional impulsive rats suggested that the subregions of OFC played the same role in decisional impulsivity. Moreover, more neurons expressed c-Fos in the NAcC in LI than in HI rats, indicating that the NAcC was more crucial than NAcS in decisional impulsivity. Thus, NAcC was considered as the key subregion of NAc for the following experiments in trait-like decisional impulsivity.

Significant difference in the activated neuronal projections from mOFC to NAcC between HI and LI rats

To investigate whether the mOFC- or lOFC-NAcC pathways contributed to the decisional impulsive behaviors, the FG was microinjected bilaterally into NAcC (Fig. 3a and Online Resource 1_Fig. S2). The FG was retrogradely traced in the somas of neurons in mOFC or lOFC two weeks later. The c-Fos/FG/NeuN triple-positive cells were counted in mOFC and lOFC, which regarded as the activated neural projections from mOFC or lOFC to NAcC in delay-discounting task performance. Unexpectedly, Qualitative results showed that more FG positive cells were detected in mOFC than in lOFC in all rats, but not in the NAcC (Fig. 3b and Online Resource 1_Table 1, Fig. S3). Besides, the number of c-Fos/FG/NeuN triple-positive cells (per mm^2) in the mOFC in LI group was much higher than that in HI group (LI, 128.8 ± 18.8; HI, 70.6 ± 13.3, Fig. 3c, d). However, there was no significant difference in the number of c-Fos/FG/NeuN triple-positive cells (per mm^2) in the lOFC between LI and HI rats (LI, 46.7 ± 8.9; HI, 42.4 ± 7.2; Fig. 3e, f). The difference in activated neural projections from mOFC to NAcC between trait-like decisional impulsive rats suggested only the mOFC-NAcC, but not the lOFC-NAcC pathway, contributed to decisional impulsive behavior.

The difference in information communication of mOFC-NAcC pathway controlled the trait-like decisional impulsive behavior

In vivo multi-channel recording was used to explore how the mOFC-NAcC pathway involved in it in free-moving trait-like decisional impulsive rats. One edited video of an example of free-trial choice in Block 4 in a HI rat was displayed in the Online Resource_Video. Each trial was divided into five windows, which reflected different states of rats in making impulsive decision: (1) the Pre-CL window (2 s before the house light on) reflected the basal condition of each choice; (2) Pre-LO window (2 s before the levers out) reflected the expected choice of large-delayed or small-immediate reward; (3) Pre-LP window (time between the lever out and lever press) reflected action

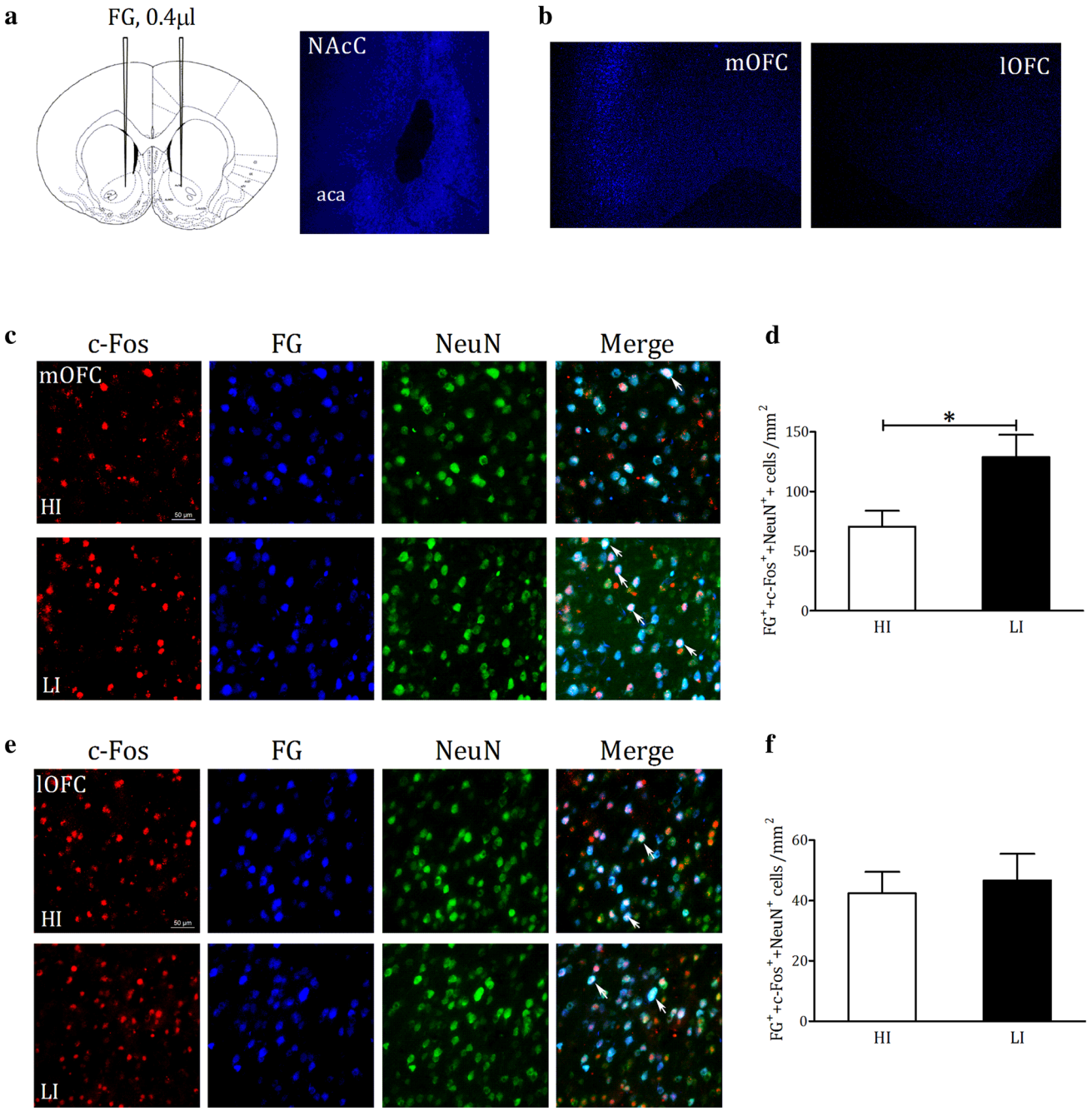

Fig. 3 Difference of activated projections from mOFC or lOFC to NAcC between HI and LI rats. **a** FG injection sites in the NAcC. **b** The number of FG positive cells in the mOFC was significantly more than that in the lOFC. Representative photomicrographs (20X) of c-Fos (red), FG (blue) and NeuN (green) labeling in the **c** mOFC or **e** lOFC in HI and LI rats after delay discounting task. Scale bar, 50 μm. Above: HI rats; Below: LI rats. Arrow: examples of c-Fos+FG+NeuN triple-positive cells. **d** The number of c-Fos+FG+NeuN triple-positive cells per mm^2 in the mOFC in LI rats was significantly more than that in HI rats (unpaired *t* test, $p < 0.05$). **f** The number of FG+c-Fos+NeuN triple-positive cells per mm^2 in the lOFC had no difference between HI and LI rats (unpaired t test, $p = 0.71$). HI and LI rats, n = 4, respectively. *$p < 0.05$, error bars represent mean ± SEM

on the levers; (4) Delay window (time between the lever press and reward delivery) reflected the reward's delay time evaluating; (5) Post-RWD window reflected reward enjoying (1 s after reward delivery) (Fig. 4a). The gPDC values of each window in different frequency oscillations were calculated to investigate the difference in information communication of mOFC-NAcC pathway between HI and LI rats.

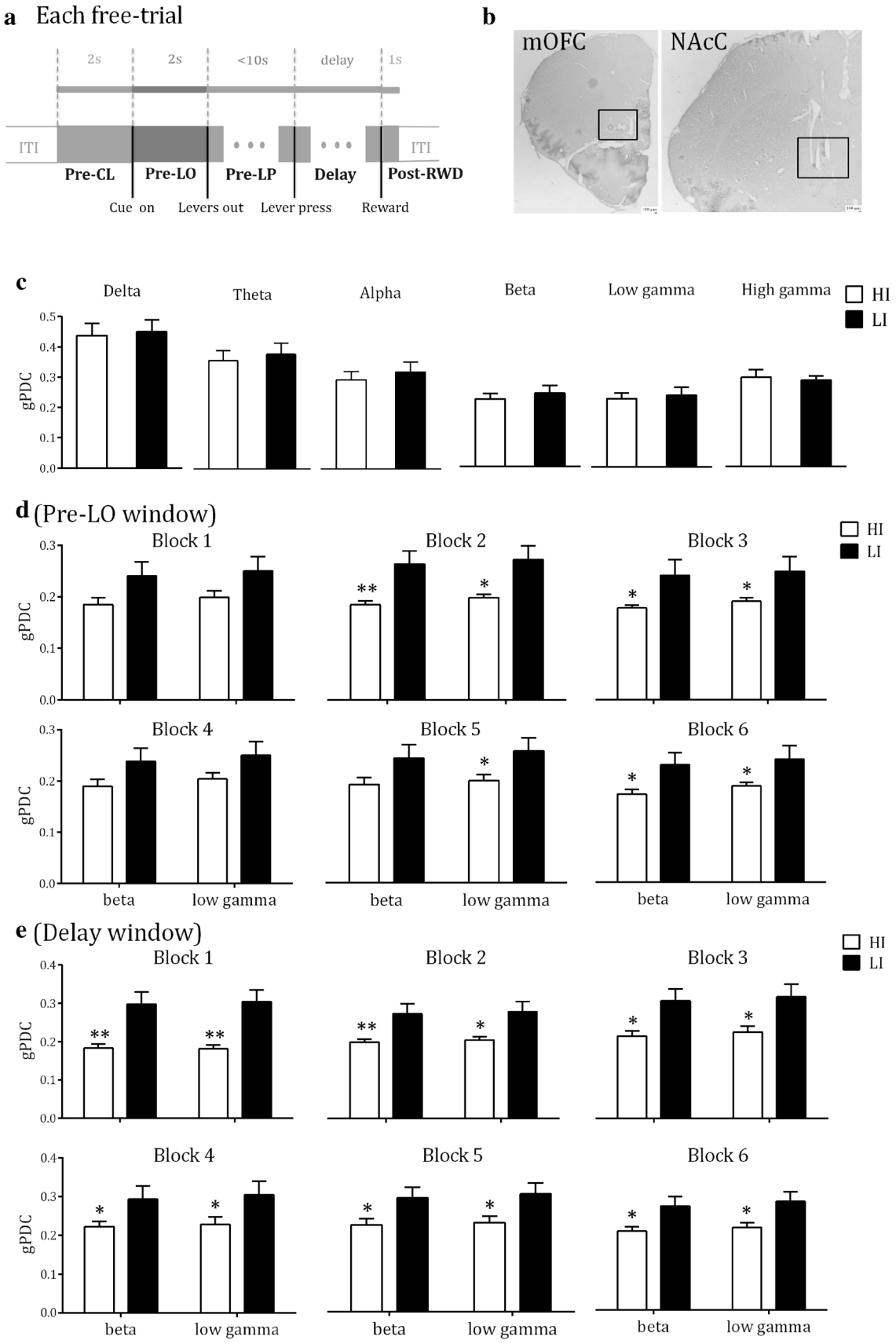
a Each free-trial
2s
2s
<10s
delay
1s
ITI
ITI
Pre-CL
Pre-LO
Pre-LP
Delay
Post-RWD
Cue on
Levers out
Lever press
Reward
b
mOFC
NAcC
c
Delta
Theta
Alpha
Beta
Low gamma
High gamma
HI
LI
gPDC
d (Pre-LO window)
Block 1
Block 2
Block 3
Block 4
Block 5
Block 6
beta
low gamma
e (Delay window)

◂**Fig. 4** Difference of the information communication of mOFC-NAcC pathway in beta and low gamma bands between HI and LI rats in the Pre-LO and Delay window. **a** Divided time windows in each free trial in delay discounting task, and time windows of multichannel data analysis. Pre-CL: 2 s before the house light on; Pre-LO: 2 s before the levers out; Pre-LP: time between the lever out and lever press; Delay: time between the lever press and reward delivery; Post-RWD: 1 s after reward delivery. **b** Schematic positions of multichannel electrode tips in the mOFC and NAcC (2.5X). **c** No significant difference in gPDC values of the mOFC-NAcC pathway in different frequency bands between HI and LI rats before the task starting (unpaired t test, delta, $p = 0.82$; theta, $p = 0.68$; alpha, $p = 0.57$; beta, $p = 0.55$; low gamma, $p = 0.61$; high gamma, $p = 0.73$). **d** The gPDC values of the mOFC-NAcC pathway in beta and low gamma bands of LI rats were significantly higher than that of HI rats in the Pre-LO window in the blocks with delay of 4 s, 8 s, 12 s, 16 s and 20 s. **e** The gPDC values of the mOFC-NAcC pathway in beta and low gamma bands of LI rats were significantly higher than that of HI rats in the Delay window in all blocks. HI rats, n = 13, LI rats, n = 13. * $p < 0.05$, ** $p < 0.01$, error bars represent mean ± SEM

The trait-like decisional impulsive rats showed their inherent characteristics during the multichannel data acquisition. The HI rats preferred small-immediate reward, whereas the LI rats preferred large-delayed reward with the increased delay of large-reward. What's more, there was no significant difference in operating rate between the two groups throughout all free trials (Online Resource 1_Fig. S4a-c).

Results showed that the gPDC values of mOFC-NAcC pathway had no significant difference in each frequency band between HI and LI rats before the delay-discounting task starting (Figs. 4c, 5a), indicating that there was no difference in information communication of the mOFC-NAcC pathway between trait-like decisional impulsive rats under basal condition. In the mentioned five windows above, the gPDC values of mOFC-NAcC pathway showed different results. Figure 4d showed that the gPDC values of mOFC-NAcC pathway in beta and low gamma oscillations of LI rats were much higher than that of HI rats across all blocks in the Pre-LO window (specific values of HI and LI rats showed in Online Resource 1_Table 3). Particularly, in Pre-LO window of Block 6, the gPDC values of mOFC-NAcC pathway in all oscillations were shown in Fig. 5b, c. What's more, the gPDC values in beta and low gamma oscillations of LI rats were much higher than that of HI rats in Delay window across all blocks (Fig. 4e, specific values shown in Online Resource 1_Table 4), and the gPDC values in all oscillations in Delay window of Block 1 were shown in Fig. 5d, e. However, in the Pre-CL window (specific values in Online Resource 1_Table 5), Pre-LP window (specific values in Online Resource 1_Table 6) and Post-RWD window (specific values in Online Resource 1_Table 7), the gPDC values of mOFC-NAcC pathway had no significant difference between HI and LI rats.

Together, these results showed in the Pre-LO and Delay window, there was significant difference in the information communication of mOFC-NAcC pathway in beta and low gamma oscillations (15-46 Hz) between trait-like decisional impulsive rats, indicating that the mOFC-NAcC pathway involved in trait-like decisional impulsivity via the expected reward encoding and delay time evaluating.

Fig. 5 Examples of gPDC values of the mOFC-NAcC pathway in all bands in HI and LI rats in the baseline, the Pre-LO and Delay window. **a** Example graph of gPDC values of the mOFC-NAcC pathway of both HI and LI rats before the task starting. **b** The gPDC values of the mOFC-NAcC pathway only in beta and low gamma bands of LI rats were significantly higher than that of HI rats in the Pre-LO window in Block 6. **c** Example graph of gPDC values of the mOFC-NAcC pathway of both HI and LI rats in the Pre-LO window in Block 6. **d** The gPDC values of mOFC to NAcC only in beta and low gamma bands of LI rats were significantly higher than that of HI rats in the Delay window in Block 1. **e** Example graph of gPDC values of the mOFC-NAcC pathway of both HI and LI rats in the Delay window in Block 1. Example graphs of **a**, **c** and **e**: left, HI; right, LI. HI rats, $n = 13$, LI rats, $n = 13$. *$p < 0.05$, **$p < 0.01$, error bars represent mean ± SEM ▸

The trait-like decisional impulsive behaviors were reversed by the specific intervention of the mOFC-NAcC pathway

To further determine the top-down control role of mOFC-NAcC pathway in regulating the trait-like decisional impulsivity, a designer receptor exclusively activated by designer drugs (DREADD)-based strategy (Mahler et al. 2014) was designed to remotely control the activation of mOFC neurons in vivo and manipulate the mOFC–NAcC pathway of HI and LI rats, respectively. The CNO/saline was microinjected bilaterally into the NAcC to activate the mOFC terminals of HI rats or not (Fig. 6a), or inactivate the mOFC terminals of LI rats (Fig. 6e). The virus infected the majority of cells in the mOFC, and highly expressed in the NAcC where the axons of the mOFC neurons located (Fig. 6b, f).

CNO pretreatment increased the choice percentage of large reward in HI rats with hM3Dq expression compared to the hM3Dq-vehicle or mCherry-CNO group (Fig. 6c), and Bonferroni post-tests showed significant difference at 8 s and 12 s. However, the operating rate of HI rats in each group did not alter (Fig. 6d). In contrast, CNO injections decreased the choice percentage of large reward in LI rats with hM4Di expression compared to the hM4Di-vehicle or mCherry-CNO group (Fig. 6g), and Bonferroni post-tests showed significant difference at 12 s, 16 s and 20 s. Similarly, the operating rate of LI rats in each group did not alter after CNO or vehicle injections (Fig. 6h). These results indicated that activating the mOFC-NAcC pathway decreased the decisional impulsivity of HI rats, whereas inhibiting this pathway could increase the decisional impulsivity of LI rats, which further proved that the mOFC-NAcC pathway regulated the decisional impulsive choice.

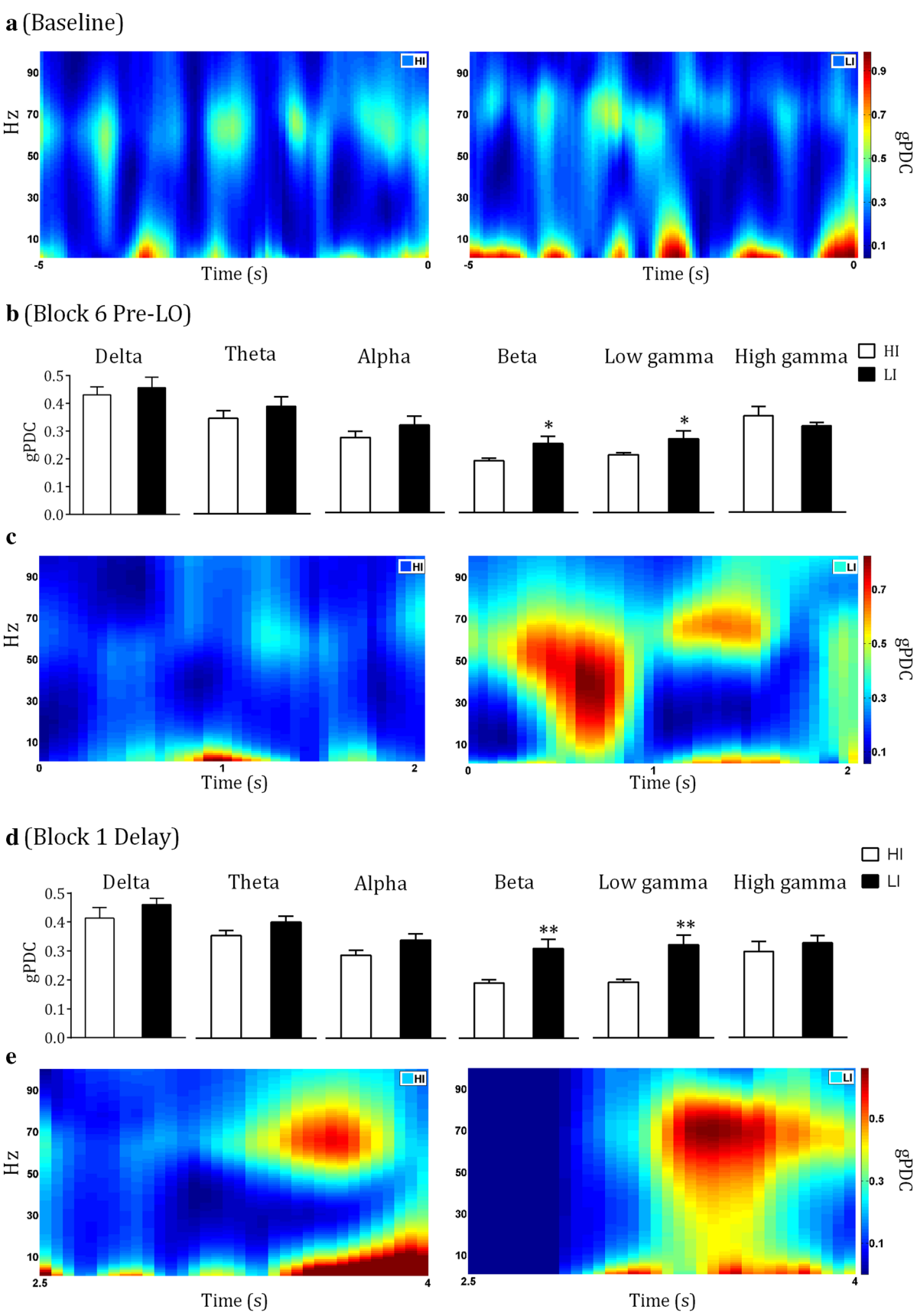
a (Baseline)
HI
LI
Hz
Time (s)
gPDC
b (Block 6 Pre-LO)
Delta
Theta
Alpha
Beta
Low gamma
High gamma
HI
LI
gPDC
c
d (Block 1 Delay)
e

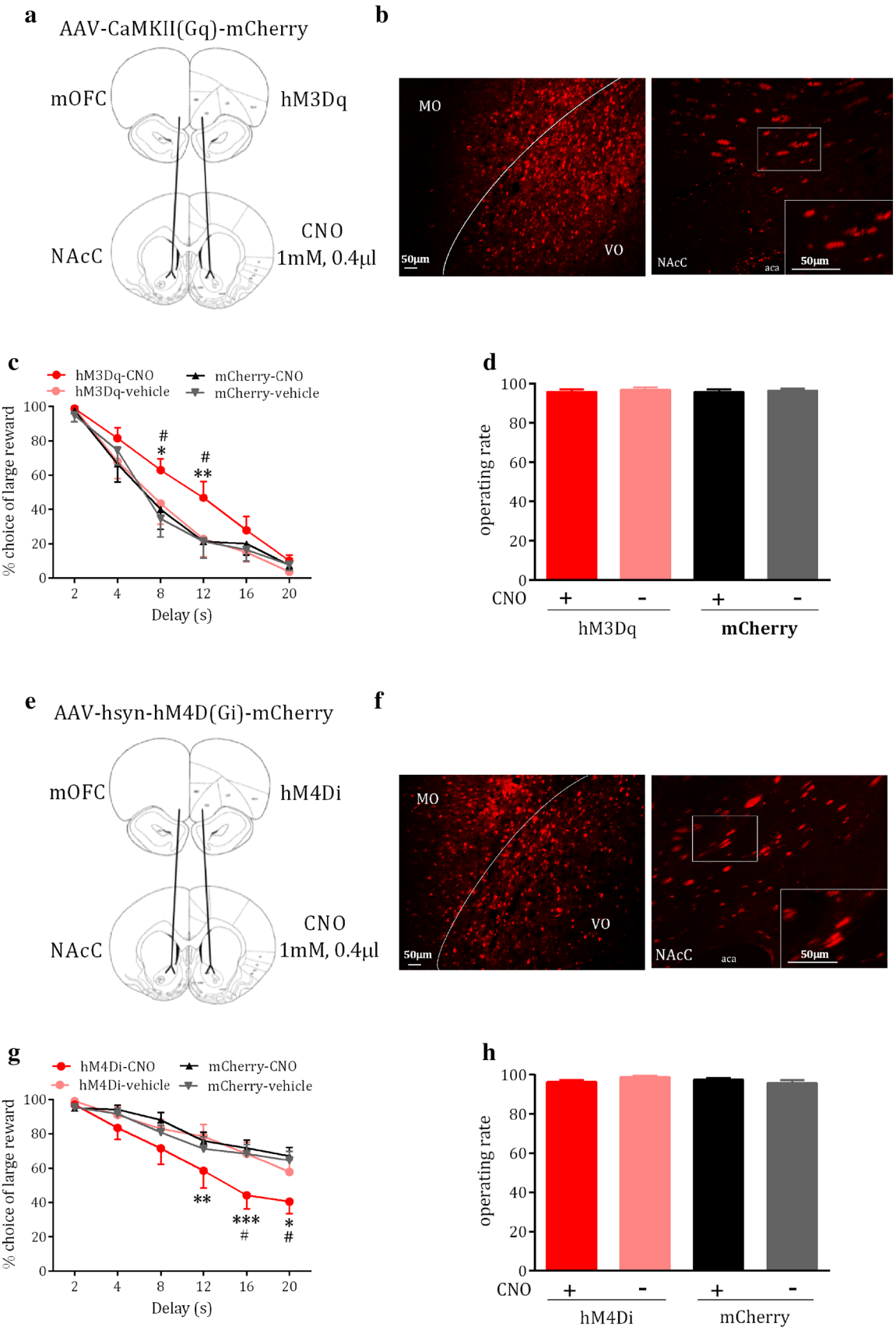
a
AAV-CaMKII(Gq)-mCherry
mOFC
hM3Dq
NAcC
CNO
1mM, 0.4μl
b
MO
VO
50μm
NAcC
aca
50μm
c
hM3Dq-CNO
hM3Dq-vehicle
mCherry-CNO
mCherry-vehicle
% choice of large reward
Delay (s)
d
operating rate
CNO
hM3Dq
mCherry
e
AAV-hsyn-hM4D(Gi)-mCherry
mOFC
hM4Di
NAcC
CNO
1mM, 0.4μl
f
MO
VO
50μm
NAcC
aca
50μm
g
hM4Di-CNO
hM4Di-vehicle
mCherry-CNO
mCherry-vehicle
% choice of large reward
Delay (s)
h
operating rate
CNO
hM4Di
mCherry

◂**Fig. 6** Activating or inhibiting the mOFC-NAcC projections reversed the impulsive behaviors of HI and LI rats with DREADDs. Projections from the mOFC to NAcC were transiently **a** activated or **e** inactivated by microinjection of CNO in the NAcC among mOFC axon terminals expressing hM3Dq or hM4Di receptors. Representative of DREADD expression in the experimental groups 5 weeks after **b** AAV5-CaMKII-hM3D(Gq)-mCherry or **f** AAV8-hSyn-hM4D(Gi)-mCherry microinjected in the mOFC. Top: typical photomicrographs (10X) for mCherry-tagged hM3Dq or hM4Di (red) in the mOFC. Bottom, Example (10X) of axonal labeling for the mCherry-tagged hM3Dq or hM4Di receptors (red) in the NAcC; Bottom right corner (40X). **c** Choice percentage of large reward of hM3Dq-CNO HI rats increased with the delay increasing, compared to hM3Dq-vehicle or mCherry-CNO HI rats (two-way ANOVA, interaction: drug × delay, $F5, 75 = 1.12$, $p = 0.16$ or $F5, 75 = 1.64$, $p = 0.16$; drug: $F1, 15 = 69.77$, $p < 0.001$ or $F1, 15 = 67.91$, $p < 0.001$; delay: $F5, 75 = 2.9$, $p < 0.001$ or $F5, 75 = 2.91$, $p < 0.001$), and Bonferroni post tests showed significant difference at 8 s and 12 s (8 s, $p < 0.05$; 12 s, $p < 0.01$ or 8 s, $p < 0.05$; 12 s, $p < 0.05$). **d** The operating rate of HI rats in each group did not affect for CNO or vehicle (one-way ANOVA, $F3, 93 = 0.19$, $p = 0.90$). **g** Choice percentage of large reward of hM4Di-CNO LI rats decreased with the delay increasing, compared to hM4Di-vehicle or or mCherry-CNO LI rats (two-way ANOVA, interaction: drug × delay, $F5, 95 = 1.9$, $p < 0.05$ or $F5, 85 = 3.76$, $p = 0.15$; drug: $F1, 19 = 37.75$, $p < 0.001$ or $F1, 17 = 36.2$, $p < 0.001$; delay: $F5, 95 = 6.21$, $p < 0.001$ or $F5, 75 = 9.76$, $p < 0.001$), and Bonferroni post tests showed significant difference at 12 s, 16 s and 20 s (12 s, $p < 0.01$; 16 s, $p < 0.001$, 20 s, $p < 0.05$ or 16 s, $p < 0.05$, 20 s, $p < 0.05$). **h** The operating rate of LI rats in each group did not affect for CNO or vehicle (one-way ANOVA, $F3, 108 = 1.71$, $p = 0.18$). Each group of HI rats, $n = 8$, respectively. hM4Di-CNO and hM4Di-vehicle LI rats, $n = 10$, respectively; mCherry-CNO and mCherry-vehicle LI rats, $n = 8$, respectively. $^{*}p < 0.05$, $^{**}p < 0.01$, $^{***}p < 0.001$, compared to hM3Dq-vehicle HI rats or hM4Di-vehicle LI rats; $\#p < 0.05$, compared to mCherry-CNO HI rats or mCherry-CNO LI rats, error bars represent mean ± SEM

Discussion

The present study revealed that more activated neurons of the mOFC, lOFC and NAcC were found in LI than HI rats, indicating that the entire OFC and NAcC were involved in decisional impulsivity. Moreover, the neuronal projection activity, information communication and chemogenetic intervention of the mOFC-NAcC pathway suggested that the mOFC-NAcC, but not lOFC-NAcC pathway was critical in controlling decisional impulsive behaviors via the expected reward encoding and its delay time evaluating. To the best of our knowledge, this is the first report that the mOFC-NAcC pathway drives a top-down control in decisional impulsivity.

Specifically, LI rats showed more c-Fos positive neurons in the mOFC and lOFC than the HI rats, implying the mOFC and lOFC played similar roles in decisional impulsivity. This finding was consistent with previous reports that patients and rats with whole OFC damage all displayed preference toward small-immediate reward and increased decisional impulsivity (Bechara et al. 2000; Berlin et al. 2004; Kheramin et al. 2003; Mobini et al. 2002; Rudebeck et al. 2006). However, our results were also inconsistent with other study that the whole OFC lesion in rats made them prefer the delayed rewards (Winstanley et al. 2004). Rats with lesions to the mOFC were more likely to choose the large-delayed reward, while rats with lesions to the lOFC preferred the small immediate reward (Mar et al. 2011), indicating that the mOFC and lOFC played opposite roles in decisional impulsivity. The contradictory results might be due to the reason that quinoline acid (QA) microinjection could cause a wide, unselective and longtime influence on the neurons and make them death. The c-Fos is one of the immediate early genes and has been proven to transcribe and express rapidly in the presence of 15 min (Hu et al. 1994), which is a classic and accurate reflection of the excitability of neurons. In the present work, the number of c-Fos positive neurons was measured to indicate whether the neurons were activated during the behavioral performance. We found that both in the mOFC and lOFC displayed significant difference in the number of activated neurons between HI and LI rats, suggesting that mOFC and lOFC played similar roles in impulsive choice behaviors, and there was a negative correlation between the number of activated neurons and the level of decisional impulsivity. The more activated neurons in the OFC there were, the lower the level of decisional impulsivity in rats was.

Additionally, the difference in the number of activated neurons between HI and LI rats in the NAcC, but not NAcS that was also consistent with previous reports. The excitatory lesions to NAcC neurons increased the choice of small-immediate reward, while the lesions to NAcS neurons did not affect the impulsive choice behaviors in rats (Paloyelis et al. 2010; Pothuizen et al. 2005; Valencia-Torres et al. 2012). Obviously, our results further confirmed that the NAcC played the vital role in decisional impulsivity. In addition, previous studies have demonstrated that the NAc is heavily innervated by glutamatergic afferents from the prefrontal cortex, including the OFC (Groenewegen et al. 1999; Asher and Lodge 2012). Similar as this study, we found that the projections existed between the mOFC and NAcC, as well as the lOFC and NAcC, and more afferent fibers from the mOFC to NAcC than from the lOFC to NAcC were detected using neuronal retrograde tracing. Moreover, the difference in the level of activation of mOFC–NAcC, but not the lOFC-NAcC projections between HI and LI rats implied that the mOFC-NAcC pathway played a more important role in controlling the decisional impulsive behavior. This point was further confirmed in our work by the chemogenetic intervention experiments that specific activation in HI rats or inhibition in LI rats of the mOFC-NAcC pathway partially reversed their decisional impulsive behaviors. These findings revealed a negative correlation between the activation level of mOFC-NAcC projections and the decisional impulsivity level. This did not conflict with previous findings that the integrity of white matter fiber structure of the frontal cortex

and striatum could predict the level of human decisional impulsivity-higher fiber bundle integrity was associated with lower decisional impulsivity (Peper et al. 2013).

Electrophysiological results in this study showed that the difference in gPDC values of mOFC-NAcC pathway between HI and LI rats occurred in the expected reward choice and delay time windows in all Blocks. In Block 1, large and small reward delays were both 2 s, and both the HI and LI rats chose the large reward. In Block2-6, the small reward delays were 2 s, and the large reward delays were 4 s, 8 s, 12 s, 16 s, and 20 s, respectively; the HI rats more chose the small immediate rewards and LI rats more chose the large delay rewards. The behavioral and electrophysiological results together reflected their different inherent characteristics in the same and different expected reward encoding and delay time evaluating. However, there was no difference in the information communication of mOFC-NAcC pathway between HI and LI rats before the delay-discounting task starting, indicating that their different inherent characteristics depended on the delay-discounting task. What's more, the difference in expected reward encoding and delay time evaluating might be the potential mechanism of mental disease, such as addiction. High-level decisional impulsive individuals are easier to relapse to drugs, who search for the immediate small reward-addictive substances instead of standing the delay of large reward, for example, good health, family happiness (Wang et al. 2016, 2018).

Moreover, reward processing is carried out by extensive fronto-subcortical network, composed with multi-brain structures including the striatum, amygdala and orbitofrontal cortex (Camara et al. 2009; Koob and Volkow 2010). Neuronal oscillations are considered to be an optimal integration mechanism that allows the coordination of the network involved in that (Courtemanche et al. 2003; Buzsáki and Draguhn 2004; Jenison 2014; Fatahi et al. 2018). However, the specific oscillations to synchronize these different structures involved in reward processing are unclear so far. A few studies have showed that the high (beta and gamma) oscillations of OFC are involved in the reward process. Increase in power in beta oscillations (13-25 Hz) of the OFC is relevant to the reward value encoding in the borderline personality disorder (BPD) patients whose reward processing have proved to be impaired (Andreou et al. 2015) and the patients with OFC lesions in an impulsive task (Solbakk et al. 2014). Combined with present results that the difference in neuron activation in the OFC between trait-like decisional impulsive rats, the number of activated mOFC neurons in expected reward encoding and delay time evaluating might be different, and resulting in the difference in information communication of the mOFC-NAcC pathway in beta and low gamma oscillations between trait-like decisional impulsive rats.

Limitations

The present study first demonstrated that the mOFC-NAcC pathway mediated top-down control in decisional impulsive behavior via the expected reward encoding and delay time evaluating. However, there were still some limitations. First, this study lacked the MI control rats, which could reflect a general level of decisional impulsivity. Second, the control of gPDC was absent that could provide powerful evidence to verify the top-down control role of mOFC-NAcC pathway.

Conclusion

In conclusion, the present study demonstrated that the subregions of OFC, mOFC and lOFC played similar roles in decisional impulsivity. Moreover, the mOFC-NAcC, but not the lOFC-NAcC pathway specifically played a top-down control role in decisional impulsive behavior. These findings not only provide a new neural physiological basis to elucidate decisional impulsive behavior, but also point out a more specific neuronal pathway for mental disorders associated with decisional impulsivity.

Funding This study was funded by the National Basic Research Program (Grant number 2015CB553500), the National Natural Science Foundation (Grant number 81471353) and Science Fund for Creative Research Groups from the National Natural Science Foundation (81521063) of China to CL Cui.

Compliance with ethical standards

Conflict of interest The authors declare that they have no conflict of interest.

Ethical approval All procedures performed in studies involving animals were in accordance with the ethical standards of the institution or practice at which the studies conducted.

Informed consent Informed consent obtained from all individual participants included in the study.

References

Andreou C, Kleinert J, Steinmann S, Fuger U, Leicht G, Mulert C (2015) Oscillatory responses to reward processing in borderline personality disorder. World J Biol Psychiatry 16(8):575–586. https://doi.org/10.3109/15622975.2015.1054880

Asher A, Lodge DJ (2012) Distinct prefrontal cortical regions negatively regulate evoked activity in nucleus accumbens subregions. Int J Neuropsychopharmacol 15(9):1287–1294. https://doi.org/10.1017/S146114571100143X

Baccalá LA, Sameshima K (2001) Overcoming the limitations of correlation analysis for many simultaneously processed neural

structures. Prog Brain Res 130:33–47. https://www.sciencedirect.com/science/article/pii/S0079612301300043?via%3Dihub
Bechara A, Tranel D, Damasio H (2000) Characterization of the decision-making deficit of patients with ventromedial prefrontal cortex lesions. Brain 123(Pt 11):2189–2202. https://academic.oup.com/brain/article/123/11/2189/255844
Berlin HA, Rolls ET, Kischka U (2004) Impulsivity, time perception, emotion and reinforcement sensitivity in patients with orbitofrontal cortex lesions. Brain 127(Pt 5):1108–1126. https://academic.oup.com/brain/article/127/5/1108/303095
Besson M, Belin D, McNamara R, Theobald DE, et al (2010) Dissociable control of impulsivity in rats by dopamine d2/3 receptors in the core and shell subregions of the nucleus accumbens. Neuropsychopharmacology 35(2):560–569. https://www.nature.com/articles/npp2009162
Bezzina G, Cheung TH, Asgari K, Hampson CL et al (2007) Effects of quinolinic acid-induced lesions of the nucleus accumbens core on inter-temporal choice: a quantitative analysis. Psychopharmacology 195(1):71–84. https://doi.org/10.1007/s00213-007-0882-0
Buzsáki G, Draguhn A (2004) Neuronal oscillations in cortical networks. Science 304(5679):1926–1929. http://www.sciencemag.org/cgi/pmidlookup?view=long&pmid=15218136
Camara E, Rodriguez-Fornells A, Ye Z, Münte TF (2009) Reward networks in the brain as captured by connectivity measures. Front Neurosci 3(3):350–362. https://doi.org/10.3389/neuro.01.034.2009
Caprioli D, Sawiak SJ, Merlo E, Theobald DE et al (2014) Gamma aminobutyric acidergic and neuronal structural markers in the nucleus accumbens core underlie trait-like impulsive behavior. Biol Psychiatry 75(2):115–123. https://linkinghub.elsevier.com/retrieve/pii/S0006-3223(13)00640-9
Cardinal RN, Pennicott DR, Sugathapala CL, Robbins TW, Everitt BJ (2001) Impulsive choice induced in rats by lesions of the nucleus accumbens core. Science 292(5526):2499–2501. http://www.sciencemag.org/cgi/pmidlookup?view=long&pmid=11375482
Courtemanche R, Fujii N, Graybiel AM (2003) Synchronous, focally modulated beta-band oscillations characterize local field potential activity in the striatum of awake behaving monkeys. J Neurosci 23(37):11741–11752
Dalley JW, Mar AC, Economidou D, Robbins TW (2008) Neurobehavioral mechanisms of impulsivity: fronto-striatal systems and functional neurochemistry. Pharmacol Biochem Behav 90(2):250–260. http://www.jneurosci.org/cgi/pmidlookup?view=long&pmid=14684876
Darna M, Chow JJ, Yates JR, Charnigo RJ, et al (2015) Role of serotonin transporter function in rat orbitofrontal cortex in impulsive choice. Behav Brain Res 293:134–142. https://linkinghub.elsevier.com/retrieve/pii/S0166-4328(15)30092-9
de Brito CS, Baccalá LA, Takahashi DY, Sameshima K (2010) Asymptotic behavior of generalized partial directed coherence. Conf Proc IEEE Eng Med Biol Soc 2010(1997):1718–1721. https://ieeexplore.ieee.org/document/5626856/
Diergaarde L, Pattij T, Poortvliet I, et al (2008) Impulsive choice and impulsive action predict vulnerability to distinct stages of nicotine seeking in rats. Biol Psychiatry 63(3):301–308. https://linkinghub.elsevier.com/retrieve/pii/S0006-3223(07)00673-7
Dombrovski AY, Szanto K, Siegle GJ, Wallace ML, et al (2011) Lethal forethought: delayed reward discounting differentiates high- and low-lethality suicide attempts in old age. Biol Psychiatry 70(2):138–144. https://linkinghub.elsevier.com/retrieve/pii/S0006-3223(10)01327-2
Fatahi Z, Haghparast A, Khani A, Kermani M (2018) Functional connectivity between anterior cingulate cortex and orbitofrontal cortex during value-based decision making. Neurobiol Learn Mem 147:74–78. https://linkinghub.elsevier.com/retrieve/pii/S1074-7427(17)30199-5
Ge F, Wang N, Cui C, Li Y, Liu Y, et al (2017) Glutamatergic projections from the entorhinal cortex to dorsal dentate gyrus mediate context-induced reinstatement of heroin seeking. Neuropsychopharmacology 42(9):1860–1870. https://www.nature.com/articles/npp201714
Groenewegen HJ, Wright C, Beijer AV, Voorn P (1999) Convergence and segregation of ventral striatal inputs and outputs. Ann N Y Acad Sci 877:49–63. https://minimanuscript.com/manuscripts/convergence-and-segregation-of-ventral-st.pdf
Harvey-Lewis C, Perdrizet J, Franklin KB (2012) The effect of morphine dependence on impulsive choice in rats. Psychopharmacology 223(4):477–487. https://link.springer.com/article/10.1007%2Fs00213-012-2738-5
Hu E, Mueller E, Oliviero S, Papaioannou VE, et al (1994) Targeted disruption of the c-fos gene demonstrates c-fos-dependent and -independent pathways for gene expression stimulated by growth factors or oncogenes. EMBO J 13(13):3094–3103. https://www.ncbi.nlm.nih.gov/pmc/articles/PMC395200/
Izquierdo A, Suda RK, Murray EA (2004) Bilateral orbital prefrontal cortex lesions in rhesus monkeys disrupt choices guided by both reward value and reward contingency. J Neurosci 24(34):7540–7548. http://www.jneurosci.org/content/24/34/7540.long
Jenison RL (2014) Directional influence between the human amygdala and orbitofrontal cortex at the time of decision-making. PLoS One 9(10):e109689. http://dx.plos.org/10.1371/journal.pone.0109689
Kheramin S, Body S, Ho M, Velázquez-Martinez DN et al (2003) Role of the orbital prefrontal cortex in choice between delayed and uncertain reinforcers: A quantitative analysis. Behavioural Processes 64(3):239–250. https://linkinghub.elsevier.com/retrieve/pii/S0376635703001426
Koob GF, Volkow ND (2010) Neurocircuitry of addiction. Neuropsychopharmacology 35(1):217–238. https://doi.org/10.1038/npp.2009.110
Li Y, Zuo Y, Yu P, Ping X, Cui C (2015) Role of basolateral amygdala dopamine D2 receptors in impulsive choice in acute cocaine-treated rats. Behav Brain Res 287:187–195. https://linkinghub.elsevier.com/retrieve/pii/S0166-4328(15)00204-1
Mahler SV, Vazey EM, Beckley JT, Keistler CR, McGlinchey EM et al (2014) Designer receptors show role for ventral pallidum input to ventral tegmental area in cocaine seeking. Nat Neurosci 17(4):577–585. https://www.nature.com/articles/nn.3664
Mar AC, Walker AL, Theobald DE, Eagle DM, Robbins TW (2011) Dissociable effects of lesions to orbitofrontal cortex subregions on impulsive choice in the rat. J Neurosci 31(17):6398–6404. http://www.jneurosci.org/cgi/pmidlookup?view=long&pmid=21525280
Metin B, Roeyers H, Wiersema JR, van der Meere JJ, Gasthuys R, Sonuga-Barke E (2016) Environmental stimulation does not reduce impulsive choice in ADHD: a "pink noise" study. J Atten Disord 20(1):63–70. https://journals.sagepub.com/doi/abs/10.1177/1087054713479667?rfr_dat=cr_pub%3Dpubmed&url_ver=Z39.88-2003&rfr_id=ori%3Arid%3Acrossref.org&journalCode=jada
Mobini S, Body S, Ho MY, Bradshaw CM, Szabadi E, Deakin JF, Anderson IM (2002) Effects of lesions of the orbitofrontal cortex on sensitivity to delayed and probabilistic reinforcement. Psychopharmacology 160(3):290–298
Padoa-Schioppa C, Assad JA (2006) Neurons in the orbitofrontal cortex encode economic value. Nature 441(7090):223–226. https://www.nature.com/articles/nature04676
Paloyelis Y, Asherson P, Mehta MA, Faraone SV, Kuntsi J (2010) DAT1 and COMT effects on delay-discounting and trait impulsivity in male adolescents with attention deficit/hyperactivity disorder and healthy controls. Neuropsychopharmacology 35(12):2414–2426. https://www.nature.com/articles/npp2010124

Patros CH, Alderson RM, Kasper LJ, Tarle SJ, Lea SE, Hudec KL (2016) Choice-impulsivity in children and adolescents with attention-deficit/hyperactivity disorder (ADHD): A meta-analytic review. Clin Psychol Rev 43:162–174. https://linkinghub.elsevier.com/retrieve/pii/S0272-7358(15)00141-5

Paxinos G, Watson C (1998) The rat brain in stereotaxic coordinates, 4th edn. Academic Press, New York

Peper JS, Mandl RC, Braams BR, de Water E (2013) Delay-discounting and frontostriatal fiber tracts: a combined DTI and MTR study on impulsive choices in healthy young adults. Cereb Cortex 23(7):1695–1702. https://doi.org/10.1093/cercor/bhs163

Perry JL, Larson EB, German JP, Madden GJ, Carroll ME (2005) Impulsivity (delay-discounting) as a predictor of acquisition of IV cocaine self-administration in female rats. Psychopharmacology 178(2–3):193–201 **(The rat brain in stereotaxic coordinates)**

Pothuizen HH, Jongen-Rêlo AL, Feldon J, Yee BK (2005) Double dissociation of the effects of selective nucleus accumbens core and shell lesions on impulsive-choice behaviour and salience learning in rats. Eur J Neurosci 22(10):2605–2616. https://doi.org/10.1111/j.1460-9568.2005.04388.x

Roesch MR, Taylor AR, Schoenbaum G (2006) Encoding of time-discounted rewards in orbitofrontal cortex is independent of value representation. Neuron 51(4):509–520. https://linkinghub.elsevier.com/retrieve/pii/S0896-6273(06)00507-1

Rudebeck PH, Walton ME, Smyth AN, Bannerman DM, Rushworth MF (2006) Separate neural pathways process different decision costs. Nat Neurosci 9(9):1161–1168. https://www.nature.com/articles/nn1756

Sohn SY, Kang JI, Namkoong K, Kim SJ (2014) Multidimensional measures of impulsivity in obsessive-compulsive disorder: cannot wait and stop. PLoS One 9(11):e111739. https://doi.org/10.1371/journal.pone.0111739

Solbakk AK, Funderud I, Løvstad M, Endestad T, et al (2014) Impact of orbitofrontal lesions on electrophysiological signals in a stop signal task. J Cogn Neurosci 26(7):1528–1545. https://www.ncbi.nlm.nih.gov/pmc/articles/pmid/24392904/

Taxidis J, Coomber B, Mason R, Owen M (2010) Assessing cortico-hippocampal functional connectivity under anesthesia and kainic acid using generalized partial directed coherence. Biol Cybern 102(4):327–340

Valencia-Torres L, Olarte-Sánchez CM et al (2012) Nucleus accumbens and delay-discounting in rats: evidence from a new quantitative protocol for analysing inter-temporal choice. Psychopharmacology 219(2):271–283

Wang JK, Fan Y, Dong Y, Ma M, Ma Y et al (2016) Alterations in brain structure and functional connectivity in alcohol dependent patients and possible association with impulsivity. PLoS One 11(8):e0161956. https://doi.org/10.1371/journal.pone.0161956

Wang JK, Fan Y, Dong Y, Ma M et al (2018) Combining gray matter volume in the cuneus and the cuneus-prefrontal connectivity may predict early relapse in abstinent alcohol-dependent patients. PLoS One 13(5):e0196860. https://doi.org/10.1371/journal.pone.0196860

Weiner LP (2008) Definitions and criteria for stem cells. Methods Mol Biol 438:3–8

Winstanley CA, Theobald DE, Cardinal RN, Robbins TW (2004) Contrasting roles of basolateral amygdala and orbitofrontal cortex in impulsive choice. J Neurosci 24(20):4718–4722. http://www.jneurosci.org/content/24/20/4718.long

Zuo Y, Wang X, Cui C, Luo F, Yu P, Wang X (2012) Cocaine-induced impulsive choices are accompanied by impaired delay-dependent anticipatory activity in basolateral amygdala. J Cogn Neurosci 24(1):196–211. https://www.mitpressjournals.org/doi/abs/10.1162/jocn_a_00131?url_ver=Z39.88-2003&rfr_id=ori%3Arid%3Acrossref.org&rfr_dat=cr_pub%3Dpubmed